Science in China Series F: Information Sciences

www.scichina.com
info.scichina.com
www.springer.com/scp
www.springerlink.com

Neural FIR adaptive Laguerre equalizer with a gradient adaptive amplitude for nonlinear channel in communication systems

ZHAO HaiQuan† & ZHANG JiaShu

Key Laboratory of Signal and Information Processing of Sichuan Province, Southwest Jiaotong University, Chengdu 610031, China

To mitigate the linear and nonlinear distortions in communication systems, two novel nonlinear adaptive equalizers are proposed on the basis of the neural finite impulse response (FIR) filter, decision feedback architecture and the characteristic of the Laguerre filter. They are neural FIR adaptive decision feedback equalizer (SNNDFE) and neural FIR adaptive Laguerre equalizer (LSNN). Of these two equalizers, the latter is simple and with characteristics of both infinite impulse response (IIR) and FIR filters; it can use shorter memory length to obtain better performance. As confirmed by theoretical analysis, the novel LSNN equalizer is stable ($0 < a < 1$). Furthermore, simulation results show that the SNNDFE can get better equalized performance than SNN equalizer, while the latter exhibits better performance than others in terms of convergence speed, mean square error (MSE) and bit error rate (BER). Therefore, it can reduce the input dimension and eliminate linear and nonlinear interference effectively. In addition, it is very suitable for hardware implementation due to its simple structure.

decision feedback, nonlinear channel, adaptive equalizer, neural network, Laguerre filter

1 Introduction

It is well known that there exist some distortions for nonlinear channel in digital communication systems, such as linear distortions caused by the limited bandwidth and multi-path propagation and nonlinear distortions introduced by the non-ideal imperfect characteristic of the channel. Therefore, some equalization schemes are needed to compensate for these distortions at the receiving end, otherwise these distortions would result in high BER and even make the system unable to work[1,2]. Researches show that nonlinear equalization techniques should be adopted to availably mitigate distortions when the channel introduces severe nonlinear distortions[2,3]. During the past decades, various nonlinear equalizers have been proposed and developed. Because of powerful nonlinear processing capability, several neural networks of different architectures (such as multilayer perceptron (MLP)[4,5], radial basis function (RBF)[6−9] and recurrent neural network (RNN)[10]) have achieved better performance than linear equalizers. However, its drawbacks (com-

Received January 10, 2008; accepted October 23, 2008
doi: 10.1007/s11432-009-0148-z
†Corresponding author (email: hqzhao0815@yahoo.com.cn)
Supported partially by the National Natural Science Foundation of China (Grant No. 60971104), the Program for New Century Excellent Talents in University of China (Grant No. NCET-05-0794), and the Doctoral Innovation Fund of Southwest Jiaotong University

Citation: Zhao H Q, Zhang J S. Neural FIR adaptive Laguerre equalizer with a gradient adaptive amplitude for nonlinear channel in communication systems. Sci China Ser F-Inf Sci, 2009, 52(10): 1881–1890, doi: 10.1007/s11432-009-0148-z

plicated architecture, heavy computations, large parameter space and local minimum point) have limited its use[4−10]. To overcome the limitations of the neural networks, a series of neural FIR filters developed by Mandic[11−14] have successfully been applied in nonlinear system identification and non-stationary signal processing. These nonlinear filters have simple architecture and low computational complexity, and their nonlinear processing capability is close to that traditional neural networks. But, because of the nature of FIR architecture, the nonlinear processing capability of the neural FIR filters is limited. In order to improve the performance of the nonlinear filter, we usually increase the dimension of the input signals, which would result in an increasing number of nodes in the input layer, thus increasing computational complexity and making it hard to realize hardware. Moreover, the high orders would lead to the problem of over-parameter estimation and degradation of the performance.

To overcome these problems, two novel nonlinear adaptive equalizers are proposed in this paper based on the decision feedback architecture[3] and the Laguerre filter characteristic[15−18], namely SNNDFE and LSNN equalizers. Both performance analysis and computer simulation show that the LSNN equalizer is not only stable, but also has better performance than others in eliminating various nonlinear distortions. In addition, the memory length of input signal is also less than that of others.

2 Channel equalization model

The block diagram of a digital communication system is depicted in Figure 1. The combined effect of the transmitter filter, the transmission medium and other components are included in the 'Channel'. At kth time instance, the transmitted signal is denoted by $s(k)$. A FIR model is widely used to model a linear channel whose output at time instant k may be written as

$$s_1(k) = \sum_{i=0}^{N_f} h(i)s(k-i), \tag{1}$$

where $h(i)$ are the channel tap values, and N_f is the length of the FIR channel. The 'NL' block represents the nonlinear distortions of the symbols in the channel and its output may be expressed as

$$s_2(k) = \psi(s_1(k)), \tag{2}$$

where $\psi(\cdot)$ is a certain nonlinear function generated by the 'NL' block. The output of the channel $s_2(k)$ is corrupted by noise $\eta(k)$, usually modeled as an additive white Gaussian noise process with a zero mean and variance σ^2. This corrupted signal is received at the receiver end and is given by $r(k) = s_2(k) + \eta(k)$. And thus the $r(k)$ is passed into the equalizer which mitigates the channel effects and recovers transmitted symbol $s(k)$ or $s(k-D)$ without any error from the knowledge of the received signal samples. D is the transmission delay associated with the physical channel, and $d(k)$ denotes the desired signal, defined by $d(k) = s(k-D)$.

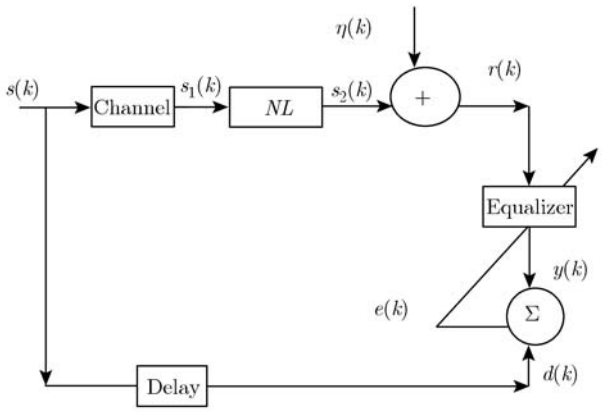

Figure 1 A digital transmission system with an equalizer.

3 Nonlinear neural adaptive equalizer

3.1 Neural FIR adaptive equalizer

To overcome the disadvantages of the complicated architecture and heavy computations in the neural networks, Mandic[11−14] developed nonlinear filters based on the FIR architecture and successfully applied them in nonlinear system identification and non-stationary signal processing. Since the nonlinear processing capability is equivalent to that of traditional neural networks, these nonlinear filters with simple architecture and low computational complexity are more suitable for nonlinear signal processing. Here, a neural FIR adaptive equalizer

based on the FIR structure (SNN) is shown in Figure 2.

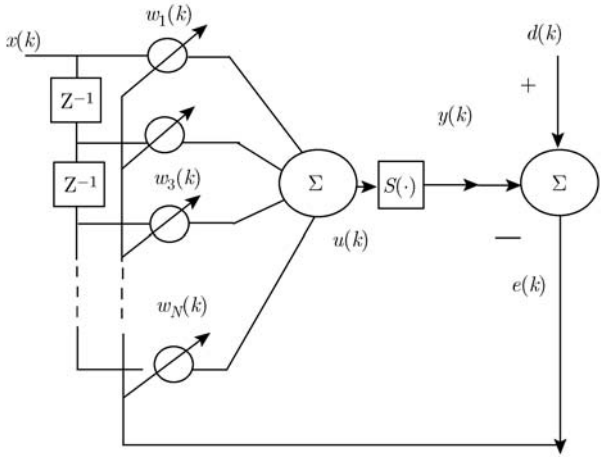

Figure 2 Diagram of a neural FIR adaptive equalizer.

The input signal vector $X(k) = [x(k)x(k-1)\cdots x(k-N+1)]^{\mathrm{T}}$ of the SNN equalizer consists of N input signals passed by the time-delay Z^{-1}. Then the output $u(k)$ of its FIR subsection is given as follows:

$$u(k) = \sum_{i=1}^{N} w_i(k)x(k-i+1) = W(k)^{\mathrm{T}}X(k), \quad (3)$$

where $W(k) = [w_1(k)w_2(k)\cdots w_N(k)]^{\mathrm{T}}$ denotes weight coefficient vector. The output $y(k)$ of this nonlinear equalizer is written as

$$y(k) = S(u(k)) = S(W(k)^{\mathrm{T}}X(k)), \quad (4)$$

where $S(\cdot)$ represents nonlinear active function and is defined by $S(u) = \frac{1}{1+\mathrm{e}^{\beta u}}$, and β is a gain parameter that controls the steep degree of the change of functional curve. To make it more suitable for various amplitude signals, we can redefine $S(u(k)) = \lambda(k)\phi(u(k))$, where parameter $\lambda(k)$ is the adjusted amplitude of the $\phi(u(k)) = \frac{1}{1+\mathrm{e}^{\beta u(k)}}$.

3.2 Neural FIR adaptive decision feedback equalizer

The decision feedback equalizer (DFE)[3], with a nonlinear architecture, can remove nonlinear distortions to a certain extent. To further effectively overcome nonlinear distortions, a novel nonlinear decision feedback equalizer (SNNDFE) is depicted in Figure 3. In Figure 3, the feedback loop denotes the feedback output signals, and these feedback signals are directly fed into the input layer of the network and are taken as part of the input signal vector $X(k)$

$$X(k) = [x(k)\ x(k-1)\cdots x(k-N_1+1)\ y(k-1)y(k-2)\cdots y(k-N_2)]^{\mathrm{T}},$$

where N_1 and N_2 stand for the lengths of input signals and feedback signals, respectively, while the length of the input signal vector $X(k)$ is $N_1+N_2 = N$. The weight update of the equalizer is controlled by the adaptive amplitude algorithm.

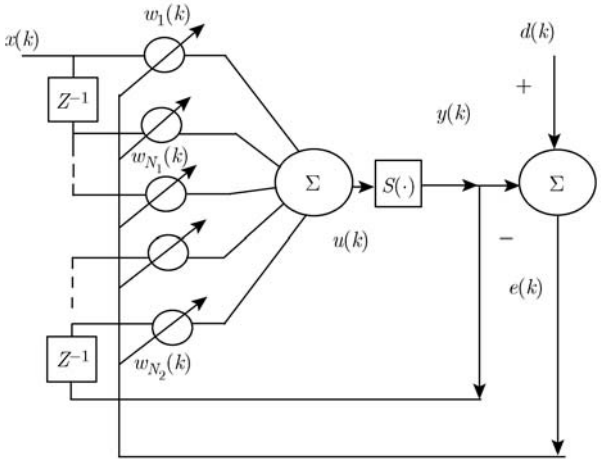

Figure 3 Diagram of the neural FIR adaptive decision feedback equalizer.

3.3 Neural FIR adaptive Laguerre equalizer

Although a decision feedback architecture can enhance nonlinear processing capability of the SNNDFE, improving the equalization performance to a certain extent, it may result in propagating errors due to the instability of its IIR structure in nature. Especially for low signal-to-noise ratio (SNR) and severe nonlinear distortions, the equalization performance may be further worsened[3].

Laguerre filter, sharing the characteristics of FIR and IIR filter, represents a compromise between computational complexity and stability. Some characteristics are listed as follows: 1) Laguerre model can efficiently describe the dynamic behavior of a wide class of systems; 2) for the estimation problem, the orthogonal property of Laguerre model offers many good performances of numerical value; 3) adaptive filter using the all-pass basis function can model long impulses of a system

with less parameters; 4) although the Laguerre filter is with an IIR structure, it can avoid the stability problem of the conventional adaptive IIR filter. For the SNN equalizer, due to the deficiency of the memory depth of the delayed Z^{-1}, it would result in high orders. On the one hand, it increases the complexity of implementation. On the other hand, it also leads to the over-parameter estimation problem of the system model. Therefore, replacing the delayed Z^{-1} of the FIR filter with the delayed section of the Laguerre in the SNN, a neural FIR adaptive Laguerre (LSNN) equalizer is proposed and depicted in Figure 4.

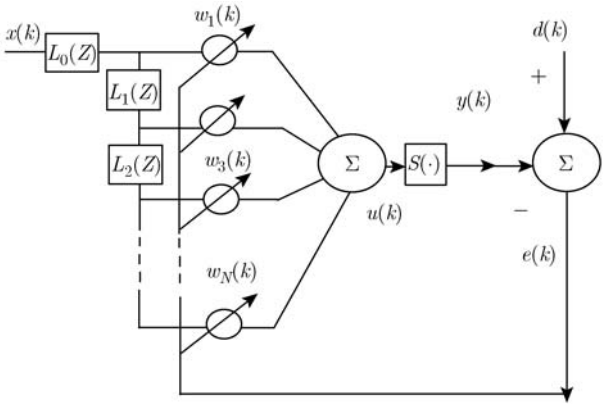

Figure 4 Neural FIR adaptive Laguerre equalizer.

Figure 4 depicts the structure of the proposed equalizer, where the delayed sections of the Laguerre filter (the memory depth > 1) consist of single pole low-pass filter network $L_0(Z)$ and all-pass filter network $L(Z)$. Moreover, these delayed networks of Laguerre filter have the IIR characteristic, whose corresponding transfer function is defined by

$$L_0(z) = \frac{\sqrt{1-a^2}}{1-az^{-1}} \quad (0<a<1), \tag{5}$$

and

$$L(z) = \frac{z^{-1}-a}{1-az^{-1}} \quad (0<a<1). \tag{6}$$

Then the transfer function of the ith delayed section of the Laguerre is given as follows:

$$L_i(z) = \sqrt{1-a^2}\frac{(z^{-1}-a)^i}{(1-az^{-1})^{i+1}} \quad i=0,1,\ldots \tag{7}$$

and Z-transform equation of eq. (7) is given by $L_i(z) = L_0(z)L^i(z)$. We can observe from eq. (7) that the LSNN equalizer is stable when $0 < a < 1$. Figure 5 illustrates the corresponding frequency response curves of the transfer function $L_i(z)$ (i=2) for the pole parameter a=0, 0.5, and 0.9. The memory depth of the model can be changed by adjusting the parameter $a(0 < a < 1)$ and will not be controlled by the filter's orders. In addition, this Laguerre filter can increase the memory depth of the low frequency part, thus filtering the information of the high frequency part. As a consequence, the memory depth of the Laguerre filter can be adjusted by changing the pole parameter a, and thereby effectively enhance the effect of filtering.

Let $l_i(m,a)$ denote the ith discrete Laguerre function:

$$l_i(m,a) = \sqrt{1-a^2}\sum_{j=0}^{i}(-1)^{i+j} \cdot C_i^{m+i-j}a^{m+i-2j}. \tag{8}$$

These discrete Laguerre functions $l_i(m,a)$ are orthonormal functions

$$\sum_{m=0}^{\infty} l_i(m,a)l_j(m,a) = \delta_{i,j} = \begin{cases} 1, & i=j, \\ 0, & i\neq j, \end{cases} \tag{9}$$

where $\delta_{i,j}$ is the Kronecker delta function. Moreover, the set formed by these Laguerre functions $l_i(m,a)$ is a complete orhtonormal set in L_2 norm. Thereby, it can also effectively improve the convergence conditions, thus speeding up the convergence speed.

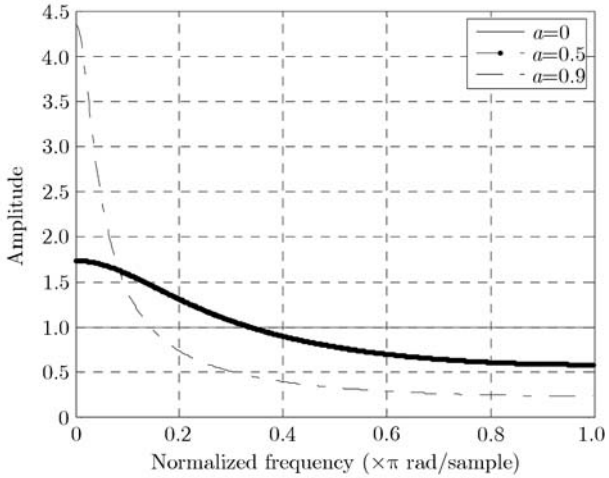

Figure 5 Frequency response curve of the transfer function $L_2(z)$.

4 Adaptive amplitude algorithm

As shown in Figure 4, the received signal $X(k)$ passes through the delayed section of the Laguerre. We can achieve a new vector $U(k) = [u_0(k), u_1(k), \ldots, u_{N-1}(k)]^{\mathrm{T}}$ as the input signal, which can be recursively computed by

$$u_0(k) = au_0(k-1) + \sqrt{1-a^2}x(k), \quad (10)$$

$$u_i(k) = u_{i-1}(k-1) + a[u_i(k-1) - u_{i-1}(k)] \ (1 \leqslant i \leqslant N). \quad (11)$$

Thus the output of the LSNN equalizer is given by

$$y(k) = S(u(k)) = S(W(k)^{\mathrm{T}}U(k)) = \lambda(k)\phi(u(k)), \quad (12)$$

where $\phi(u(k)) = \frac{2}{1+\mathrm{e}^{-2(u(k))}} - 1$, and $\lambda(k)$ denotes the amplitude of $\phi(u(k))$. For the corresponding approaches to estimating and adjusting pole parameter a, please see refs. [17–19].

According to the instantaneous error normalized least mean square (NLMS) adaptive algorithm rule, using the method of Lagrange multiplier, we can define the cost function as

$$J_k(W) = \|\Delta W(k+1)\|^2 + \beta e_1(k), \quad (13)$$

where β denotes the Lagrange multiplier, $\|\Delta W(k+1)\|^2$ represents the square operation of the Euclidean norm, and $\Delta W(k+1)$ denotes the increment of the weight coefficient: $\Delta W(k+1) = W(k+1) - W(k)$. The error $e_1(k)$ is defined by

$$e_1(k) = d(k) - \tilde{y}(k), \quad (14)$$

where

$$\tilde{y}(k) = \lambda(k)\phi(W(k+1)^{\mathrm{T}}U(k)). \quad (15)$$

To find the optimal value of the updated weight vector that makes the minimum of the cost function, the partial derivative of the $J_k(W)$ with respect to $W(k+1)$ is obtained

$$\frac{\partial J_k(W)}{\partial W(k+1)} = 2(W(k+1) - W(k)) - \beta\frac{\partial \tilde{y}(k)}{\partial W(k+1)}, \quad (16)$$

where

$$\frac{\partial \tilde{y}(k)}{\partial W(k+1)} = \lambda(k)\phi'(W(k+1)U(k))U(k). \quad (17)$$

Setting eq. (16) at zero and solving for the optimum value $W(k+1)$, we obtain

$$W(k+1) = W(k) + \frac{\beta}{2}\frac{\partial \tilde{y}(k)}{\partial W(k+1)}. \quad (18)$$

Considering the first order Talyer expansion of the function ϕ:

$$\phi(W(k+1)^{\mathrm{T}}U(k)) \approx \phi(0) + \phi'(x)|_{x=0}x \approx W(k+1)^{T}U(k), \quad (19)$$

and $\phi'(W(k+1)U(k)) \approx \phi'(W(k)U(k))$, we can substitute eq. (18) to $d(k) = \lambda(k)\phi(W(k+1)^{\mathrm{T}}U(k))$, and get

$$\begin{aligned} d(k) &= \lambda(k)W(k+1)^{\mathrm{T}}U(k) \\ &= \lambda(k)\left(W(k) + \frac{\beta}{2}\frac{\partial \tilde{y}(k)}{\partial W(k+1)}\right)U(k) \\ &= \lambda(k)\left[W(k)U(k) + \frac{\beta}{2}\frac{\partial \tilde{y}(k)}{\partial W(k+1)}U(k)\right] \\ &= \lambda(k)\phi(W(k)U(k)) \\ &\quad + \frac{\beta}{2}(\lambda^2(k)\phi'(W(k+1)U(k)))\,\|U(k)\|^2 \\ &= \lambda(k)\phi(W(k)U(k)) + \frac{\beta}{2}A(k)\,\|U(k)\|^2, \end{aligned} \quad (20)$$

where $A(k) = \lambda^2(k)\phi'(W(k)U(k))$. Then, solving for β, we can obtain

$$\beta = \frac{2e(k)}{A(k)\,\|U(k)\|^2} \quad (21)$$

and $e(k) = \lambda(k)\phi(W(k)^{\mathrm{T}}U(k))$.

Therefore, by eq. (21), we have the update equation of the weight coefficient

$$W(k+1) = W(k) + \eta_1\frac{\lambda(k)\phi'(W(k)U(k))e(k)U(k)}{A(k)\|U(k)|^2}. \quad (22)$$

When overcoming the gradient noise amplification problem, the NLMS algorithm introduces a problem of its own; that is, when the input vector $U(k)$ is small, numerical difficulties may arise because we have to divide by a small value the square norm $\|U(k)\|^2$. To overcome this problem, we modify the recursion of eq. (22) slightly to produce

$$W(k+1) = W(k) + \eta_1\frac{\lambda(k)\phi'(W(k)U(k))e(k)U(k)}{\varepsilon + A(k)\|U(k)\|^2}, \quad (23)$$

where $\varepsilon > 0$. While ε=0, eq. (23) reduces to the form given in eq. (22).

The above adaptive algorithm is summarized as follows:

$$\begin{cases} u_0(k) = au_0(k-1) + \sqrt{1-a^2}x(k), \\ u_i(k) = u_{i-1}(k-1) + a[u_i(k-1) - u_{i-1}(k)] \\ \qquad (1 \leqslant i \leqslant m), \\ e(k) = d(k) - S(W(k)^{\mathrm{T}}U(k)), \\ S(W(k)^{\mathrm{T}}U(k)) = \lambda(k)\phi(W(k)^{\mathrm{T}}U(k)), \\ A(k) = \lambda^2(k)\phi'(W(k)U(k)), \\ W(k+1) \\ = W(k) + \eta_1 \dfrac{\lambda(k)\phi'(W(k)U(k))e(k)U(k)}{\varepsilon + A(k)\|U(k)\|^2}, \\ \lambda(k+1) = \lambda(k) + \rho e(k)\phi(u(k)). \end{cases} \tag{24}$$

5 The stability analysis

The output of the LSNN equalizer is described by $y(k) = S(u(k)) = \lambda(k)\phi(u(k))$. Considering the first order Taylor expansion of $\phi(u(k))$

$$\begin{aligned} \phi(W(k)^{\mathrm{T}}U(k)) &\approx \phi(0) + \phi'(x)|_{x=0}x \\ &\approx W(k)^{\mathrm{T}}U(k) \\ &= \sum_{i=1}^{m} w_i(k)U(k-m+i), \end{aligned} \tag{25}$$

and making Z-transformation on both sides of eq. (25), we have

$$Y(Z) = \lambda(k)\sum_{i=1}^{m} w_i(k)L_i(Z)X(Z). \tag{26}$$

Therefore, the corresponding transfer function is depicted by

$$\begin{aligned} H(Z) = \frac{Y(Z)}{X(Z)} &= \lambda(k)\sum_{i=1}^{m} w_i(k)L_i(Z) \\ &= \lambda(k)\sum_{i=1}^{m} w_i(k)L_0(Z)L(Z)^i. \end{aligned} \tag{27}$$

Thereby, when $0 < a < 1$, the $H(Z)$ is stable. And the stability of equalization system is also guaranteed.

In the following, we discuss the case where step size η_1 values affect the stability of the system. According to the physical mechanism of the desired response, we have

$$d(k) = \lambda(k)\phi(W^{\mathrm{T}}U(k)) + v(k), \tag{28}$$

where W is an unknown parameter vector of the model, and $v(k)$ is an additional distortion. Weight vector $\hat{W}(k)$ computed by the NLMS algorithm is an estimation of W. Let us define estimated error of weight coefficient be

$$\varepsilon(k) = W - \hat{W}(k). \tag{29}$$

According to the recursive formulation (22) of $\hat{W}(k)$, we have

$$\begin{aligned} &\varepsilon(k+1) \\ &\quad = \varepsilon(k) - \eta_1 \frac{\lambda(k)\phi'(W(k)U(k))e(k)U(k)}{A(k)\left\|U(k)\right\|^2}. \end{aligned} \tag{30}$$

The underlying idea of an NLMS algorithm is minimizing the incremental change in the weight vector from iteration k to iteration $k+1$, subject to a constraint imposed on the updated tap-weight vector $\hat{W}(k+1)$. Therefore, taking the squared Euclidean norms of both sides of eq. (31), rearranging terms, and then taking expectations, we get

$$\begin{aligned} &E\|\varepsilon(k+1)\|^2 - E\|\varepsilon(k)\|^2 \\ &\quad = \eta_1^2 E\left[\left\| \frac{\lambda(k)\phi'(W(k)U(k))e(k)U(k)}{A(k)\|U(k)\|^2} \right\|^2\right] \\ &\quad\quad - 2\eta_1 E\left[\frac{\varepsilon(k)\lambda(k)\phi'(W(k)U(k))e(k)U(k)}{A(k)\|U(k)\|^2}\right]. \end{aligned} \tag{31}$$

From eq. (31), we easily observe that the mean-square deviation $E\|\varepsilon(k+1)\|^2$ decreases exponentially with increasing number of iterations k, and the NLMS filter is stable in the mean-square error sense (i.e., the convergence process is monotonic), provided that the normalized step-size parameter η_1 is bounded

$$\begin{aligned} &0 < \eta_1 \\ &\quad < 2\frac{E[\frac{\varepsilon(k)e(k)U(k)}{A(k)\|U(k)\|^2}]}{\lambda(k)\phi'(W(k)U(k))E[\|\frac{e(k)U(k)}{A(k)\|U(k)\|^2}\|^2]}, \end{aligned} \tag{32}$$

and we also readily find that the largest value of the mean-square deviation is achieved at the midpoint of the interval defined therein. Then the optimal step-size parameter is given by

$$\begin{aligned} \eta_{\mathrm{opt}} &= \frac{E[\frac{\varepsilon(k)e(k)U(k)}{A(k)\|U(k)\|^2}]}{\lambda(k)\phi'(W(k)U(k))E[\|\frac{e(k)U(k)}{A(k)\|U(k)\|^2}\|^2]} \\ &\approx \frac{D(k)E[U^2(k)]}{\lambda(k)\phi'(W(k)U(k))E[e^2(k)]}. \end{aligned} \tag{33}$$

Moreover, parameter $\lambda(k)$ also controls the convergence of the adaptive algorithm of this equalizer. It is our goal that $|e(k)| \to 0$ as $k \to \infty$.

The derivative of $S(u(k))$ with respect to $W(k)$ is obtained by

$$\frac{\partial S(u(k))}{\partial W(k)} = \lambda(k)\phi'(W(k)^{\mathrm{T}}U(k))U(k). \quad (34)$$

According to refs. [12, 14], we have

$$\begin{aligned} &|e(k+1)| \\ &\quad \leqslant |1-\lambda^2(k)\eta[\phi'(W(k)^{\mathrm{T}}U(k))]^2 \\ &\qquad \|U(k)\|^2|e(k)|. \end{aligned} \quad (35)$$

Hence

$$|1-\lambda^2(k)\eta[\phi'(W(k)^{\mathrm{T}}U(k))]^2\|U(k)\|^2| < 1. \quad (36)$$

To guarantee the convergence of the equalizer, we can get

$$0 < \lambda^2(k) < \frac{2}{\eta_{\mathrm{opt}}[\phi'(W(k)^{\mathrm{T}}U(k))]^2\|U(k)\|^2}. \quad (37)$$

Then, substituting eq. (33) into eq. (37), we may write

$$\begin{aligned} &0 < \lambda(k) \\ &\quad < \frac{2E[e^2(k)]D(k)}{\phi'(W(k)^{\mathrm{T}}U(k))E[U^2(k)]\|U(k)\|^2}. \end{aligned} \quad (38)$$

6 Computer simulations

To evaluate the performance of the proposed nonlinear equalizer for various nonlinear channel models[4,5], we can compare SNNDFE and LSNN with the SNN. In the simulation, the transmitted message is with 2PAM signal which is assumed to have statistically independent and equally probable values from $\{1, -1\}$. The channel output is corrupted by a zero mean additive white Gaussian noise under the SNR of 15 dB. The input lengths of the SNN and LSNN are 11 and 3, respectively. For the SNNDFE, the forward input length is 6 while the feedback length is 5.

The channel impulse response considered here is according to refs. [4, 5] as follows:

$$h(i) = \begin{cases} \frac{1}{2}\left\{1+\cos\left[\frac{2\pi}{\Lambda}(i-2)\right]\right\}, & i = 1, 2, 3, \\ 0, & \text{others}, \end{cases} \quad (39)$$

where the parameter Λ is varied from 2.9 to 3.5 in step 0.2. The value of the eigenvalue radio (EVR)[5] is given by 6.08, 11.12, 21.71, and 46.82 for Λ values of 2.9, 3.1, 3.3, and 3.5, respectively. Moreover, we can obtain the corresponding transfer function under various EVR.

$$\begin{aligned} &CH = 1 : 0.209 + 0.995z^{-1} + 0.209z^{-2}, \\ &CH = 2 : 0.260 + 0.930z^{-1} + 0.260z^{-2}, \\ &CH = 3 : 0.304 + 0.903z^{-1} + 0.304z^{-2}, \\ &CH = 4 : 0.341 + 0.876z^{-1} + 0.341z^{-2}. \end{aligned} \quad (40)$$

To study the capability of overcoming nonlinear distortions in the experiment, various nonlinear models are given

$$\begin{aligned} &NL = 0 : S_2(k) = S_1(k), \\ &NL = 1 : S_2(k) = \tanh(S_1(k)), \\ &NL = 2 : S_2(k) = S_1(k) + 0.2S_1^2(k) - 0.1S_1^3(k), \\ &NL = 3 : S_2(k) \\ &\quad = S_1(k) + 0.2S_1^2(k) - 0.1S_1^3(k) \\ &\qquad + 0.5\cos(\pi S_1(k)), \end{aligned} \quad (41)$$

where a linear channel model is represented by $NL = 0$. We can employ three nonlinear models of the linear channel $CH = 3$ in the following simulations.

6.1 The pole parameter a

Since the performance of the LSNN equalizer depends critically on the value of the pole parameter a of the tap-delayed section, the way to choose the value of pole parameter a is very important. At present, there have been some methods that can realize the choice of pole parameter a[17–19]. For instance, Silva[17] described an off-line optimization rule, but this rule would decrease the convergence speed of the nonlinear equalizer to a certain degree. In this paper, the approach in ref. [19] is adopted to choose the optimal a. According to the different a, we can get the corresponding MSEs and plot the changed curve. Figure 6 depicts the relation between the MSE and pole parameter a with the nonlinear channel model $NL = 3$ under $CH = 3$.

As is evident in Figure 6, the MSE firstly fast descends with the increasing a, and then inclines to balance, and finally begins to ascend by about 0.15 of a. Therefore, to get better performance, we can take a=0.1 as the approximating optimal solution of pole parameter a.

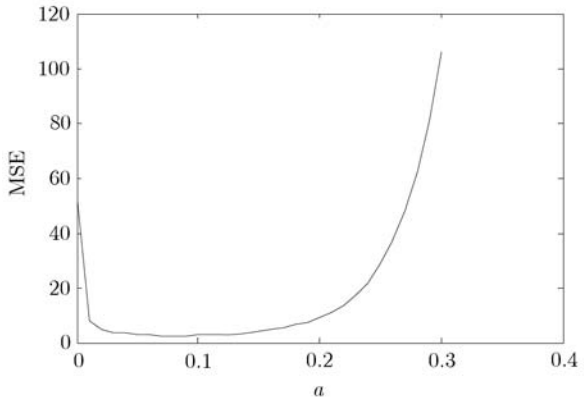

Figure 6 Relation between MSE and pole parameter a with the nonlinear channel model $NL = 3$ under $CH = 3$.

6.2 Performance of the equalizer

To illustrate the performance of our nonlinear equalizer, we can evaluate it from three aspects: convergence performance, BER performance under different SNR and the BER under different EVR.

6.2.1 Performance of the convergence. The convergence characteristics of the MSE for $CH = 3$ at SNR of 15 dB is plotted in Figure 7. In the simulation we take $CH = 3$ and SNR=15 dB, and then calculate MSE. For different linear and nonlinear channels, simulations show that the convergence rate of the LSNN equalizer is superior to that of the SNNDFE and SNN equalizers. And the convergence is much faster. As the nonlinear intensity increases, the steady-state error of three nonlinear equalizers also increases. However, the LSNN equalizer has a lower steady-state error than other equalizers all the time. In particular, for very severe nonlinear distortions (see Figure 7(d)), the MSE of the LSNN equalizer still holds about -23 dB. Simulations show that the novel adaptive equalizer can efficiently remove the different linear and nonlinear distortions.

6.2.2 BER performance under the different SNR. BER performance of the three nonlinear equalizers for $CH = 3$ for both linear and nonlinear channel

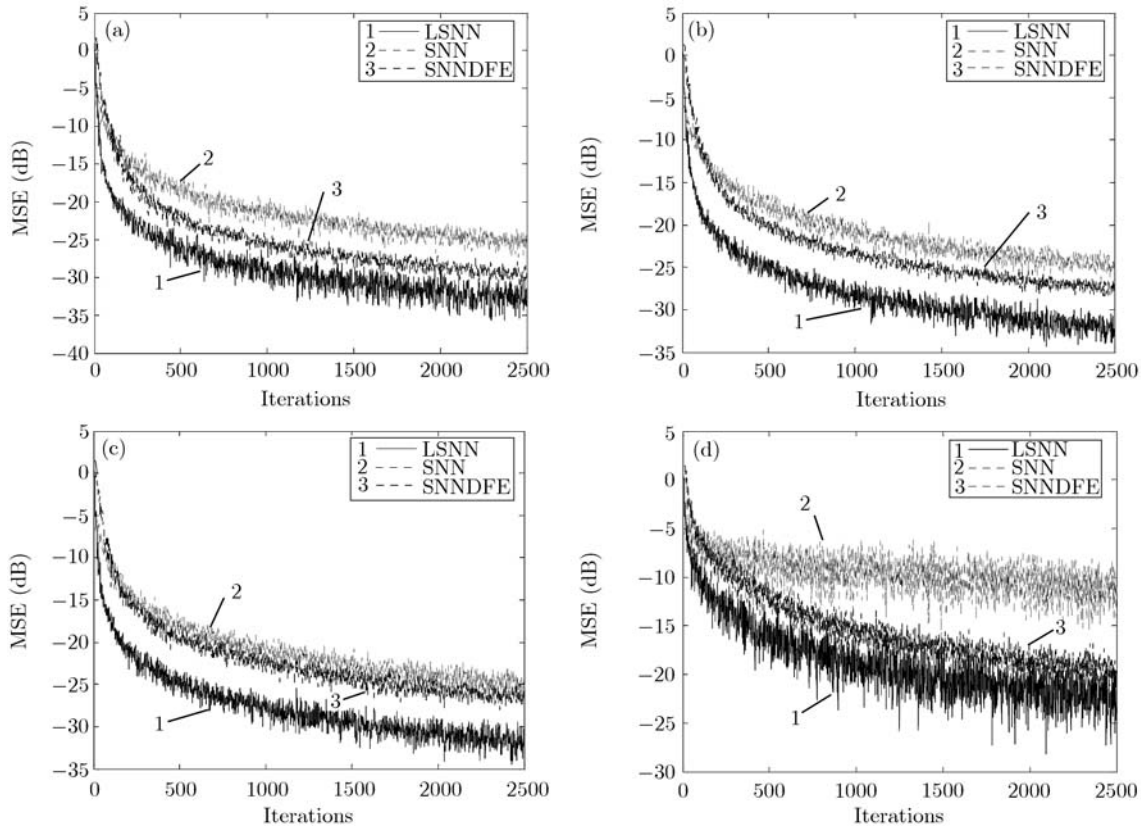

Figure 7 Convergence characteristics of the three nonlinear equalizers for $CH = 3$ with different nonlinear models at SNR of 15 dB. (a) $NL = 0$; (b) $NL = 1$; (c) $NL = 2$; (d) $NL = 3$.

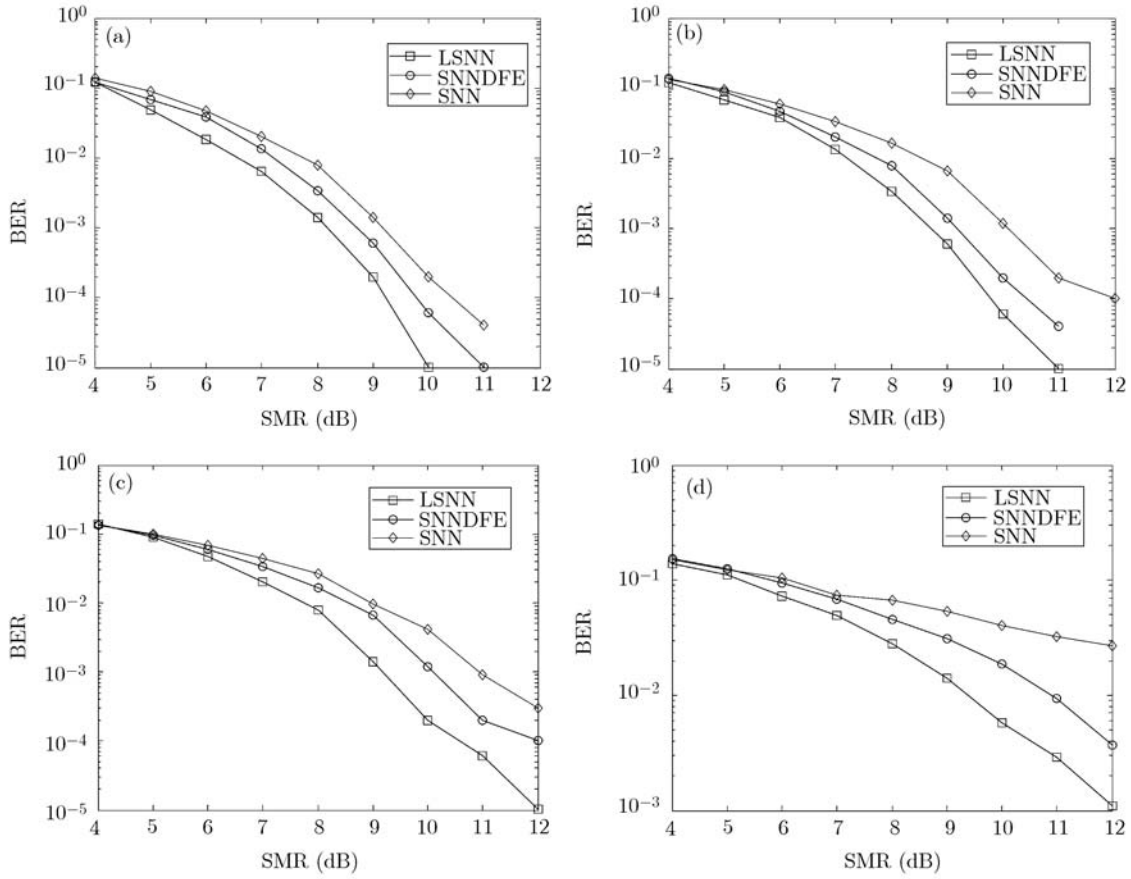

Figure 8 BER performance of the three nonlinear equalizers for $CH = 3$ with variation of SNR. (a) $NL = 0$; (b) $NL = 1$; (c) NL=2; (d) NL=3.

models is plotted in Figure 8 with SNR values varying from 4 to 12 dB for the linear ($NL = 0$) and three nonlinear channel models ($NL = 2, NL = 3$ and $NL = 4$). Though the computational complexity of the LSNN equalizer is no better than that of the SNN equalizer, as Figure 8 shows, the LSNN equalizer is superior to the SNN and SNNDFE in terms of BER performance. Especially, for severe nonlinear channel model ($NL = 3$), the LSNN outperforms others.

6.2.3 BER performance on the effect of EVR. For the three different equalizers, the effect of the variation of EVR on the BER performance of the equalizers at SNR of 10 dB is depicted in Figure 9. For all the equalizers, the BER increases with increasing EVR for both linear and nonlinear models. However, the performance degradation due to the increase of EVR is less severe in the LSNN equalizer than in other equalizers.

7 Conclusions

This paper proposes two novel adaptive equalizers to solve the nonlinear channel equalization problem in communication system. The proposed LSNN equalizer not only has simple architecture, but also shares the characteristics of IIR and FIR filter, and uses short memory length to obtain better performance. Moreover, theoretical analysis shows that the novel equalizer is stable. Furthermore, simulation results also show that SNNDFE can get better performance than SNN equalizer, while LSNN equalizer exhibits better performance than others in terms of convergence speed, MSE and BER for different linear and nonlinear channels. And its hardware implementation is very easy due to its simple structure. Therefore, it is very suitable for nonlinear channel equalization in real-time digital communication systems.

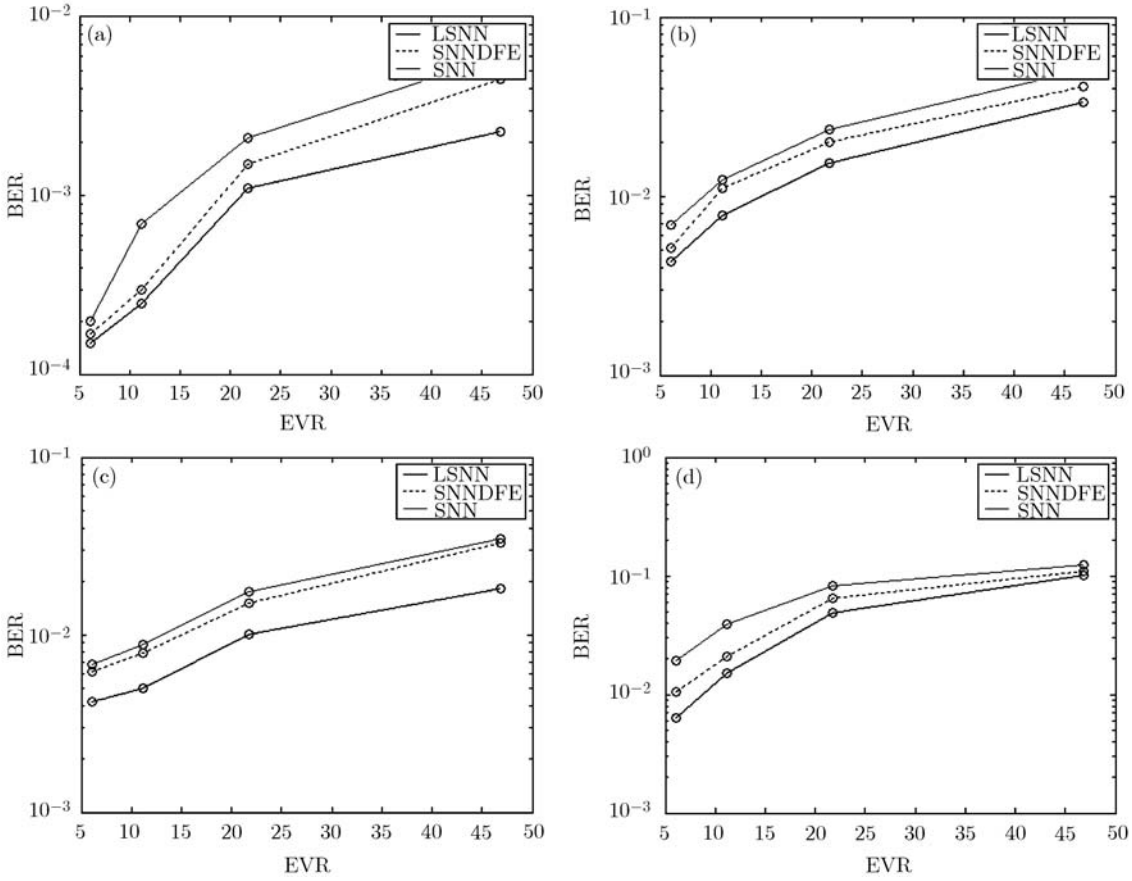

Figure 9 Effect of variation of EVR on BER performance at SNR of 10 dB. (a) NL=0; (b) NL=1; (c) NL=2; (d) NL=3.

1 Proakis J G. Digital Communications. 4th ed. New York: McGraw-Hill, 2000

2 Haykin S. Adaptive Filter Theory. 4th ed. Englewood Cliffs, NJ: Prentice-Hall, 2001

3 Qureshi S. Adaptive equalization. Proc IEEE, 1985, 73(9): 1349–1387

4 Gibson G J, Sin S, Cowan C F N. Application of multilayer perceptions as adaptive equalizer. In: Proc of IEEE Int Conf on ASSP, Glasgow, Scotland, 1989. 1183–1186

5 Gibson G J, Sin S, Cowan C F N. The application of nonlinear structures to the reconstruction of binary signals. IEEE Trans Signal Process, 1991, 39(8): 1877–1885

6 Chen S, Gibson G. J, Cowan C F N, et al. Reconstruction of binary of signals using an adaptive radial-basis-function equalizer. Signal Process, 1991, 22(1): 77–93

7 Cha I, Kassam S A. Channel equalization using adaptive complex radial basis function networks. IEEE J Select Area Commun, 1995, 13(1): 122–131

8 Chen S, Mulgrew B, Grant P M. A clustering technique for digital communication channel equalization using radial basis function networks. IEEE Trans Neural Netw, 1993, 4(4): 570–579

9 Chen S, Mulgrrew B. Overcoming co-channel interference using an adaptive radial basis function equalizer. Signal Process, 1992, 28: 91–107

10 Kechriotis G, Zervas E, Manolakos E S. Using recurrent neural networks for adaptive communication channel equalization. IEEE Trans Neural Netw, 1994, 5(2): 267–278

11 Mandic D P. NNGD algorithm for neural adaptive filters. Electron Lett, 2000, 39(9): 845–846

12 Mandic D P, Hanna A I, Razaz M. A normalized gradient descent algorithm for nonlinear adaptive filters using gradient adaptive step size. IEEE Signal Process Lett, 2001, 8(11): 295–297

13 Hanna A I, Mandic D P. Nonlinear FIR adaptive filters with a gradient adaptive amplitude in the nonlinearity. IEEE Signal Process Lett, 2002, 9(8): 253–255

14 Mandic D P, Krcmar I R. Stability of NNGD algorithm for nonlinear system identification. Electron Lett, 2001, 37(3): 200–202

15 Wahlberg B. System identification using Laguerre models. IEEE Trans Autom Control, 1991, 36: 551–562

16 Makila P M. Approximation of stable systems by Laguerre filters. Automatica, 1990, 26: 333–345

17 Silva O T. On the determination of the optimal pole position of Laguerre filters. IEEE Trans Signal Process, 1995, 43(9): 2079–2087

18 Wang L, Cluett W R. Optimal choice of time-scaling factors for linear system approximations using Laguerre models. IEEE Trans Autom Control, 1994, 39(7): 1463–1467

19 Hung F Y, Zhang J S. A novel nonlinear adaptive prediction filter for narrowband interference suppression in DS-SS communication. J Electron Inf Tech, 2007, 29(6): 1328–1331